Analysis of Bioheat Transport Through a Dual Layer Biological Media

Shadi Mahjoob

Kambiz Vafai[1]
Fellow ASME
e-mail: vafai@engr.ucr.edu

Department of Mechanical Engineering,
University of California,
Riverside, CA 92521

A comprehensive analysis of bioheat transport through a double layer and multilayer biological media is presented in this work. Analytical solutions have been developed for blood and tissue phase temperatures and overall heat exchange correlations, incorporating thermal conduction in tissue and vascular system, blood-tissue convective heat exchange, metabolic heat generation, and imposed heat flux, utilizing both local thermal nonequilibrium and equilibrium models in porous media theory. Detailed solutions as well as Nusselt number distributions are given, for the first time, for two primary conditions, namely, isolated core region and uniform core temperature. The solutions incorporate the pertinent effective parameters for each layer, such as volume fraction of the vascular space, ratio of the blood, and the tissue matrix thermal conductivities, interfacial blood-tissue heat exchange, tissue/organ depth, arterial flow rate and temperature, body core temperature, imposed hyperthermia heat flux, metabolic heat generation, and blood physical properties. Interface temperature profiles are also obtained based on the continuity of temperature and heat flux through the interface and the physics of the problem. Comparisons between these analytical solutions and limiting cases from previous works display an excellent agreement. These analytical solutions establish a comprehensive presentation of bioheat transport, which can be used to clarify various physical phenomena as well as establishing a detailed benchmark for future works in this area.
[DOI: 10.1115/1.4000060]

Keywords: bioheat transfer, biological tissue/organ, hyperthermia, porous media, multilayer media

1 Introduction

Hyperthermia treatment is recognized as one of the main cancer therapies following surgery, chemotherapy, and radiation techniques. Understanding thermal transport and temperature distribution within biological tissues and body organs are important therapeutic aspects related to this treatment [1,2]. This technique is also utilized for eradication or reduction in benign tumors, repair of sports injuries, modification and remodeling of a targeted tissue [3], gene therapy, and immunotherapy (vaccination) [4]. In hyperthermia, the tumor cells will be heated to a therapeutic value, typically 40°C–45°C, to damage or kill the cancer cells [5,6]. Although it has been known for many years that fever can damage the cancer cells, hyperthermia technique is more recently being developed as a cancer treatment by controlling and focusing the heat on the cancer cells. This technique is being utilized for several types of cancer [7].

In contrast to healthy cells, a tumor is a tightly packed body of cells in which blood circulation is restricted. Heat can cut off the oxygen and vital nutrients from the abnormal cells, resulting in a breakdown in the tumor's vascular system and destruction of the cell's metabolism and subsequent devastation of the tumor cells. In addition, heat causes the formation of certain proteins in the diseased cancer cells, the so-called heat shock proteins, which appear on the surface of the degenerated cells. The body's immune system detects these proteins as extraneous cells, making the abnormal cells visible to the immune system.

Hyperthermia technique also improves the efficiency of other cancer therapies such as chemotherapy and radiotherapy [4,8,9]. Insolated cells, which would not respond to chemotherapy or radiation alone, would be subjected to heat treatment. Hyperthermia, in conjunction with chemotherapy, causes the drug to penetrate deeper into the tumor while augmenting the efficacy of the drug delivered to the tumor. Hyperthermia treatment can be utilized either on the whole body or locally targeting the cancer cells, utilizing warm water bath balloons and blankets, hot wax, inductive coils (similar to those in electric blankets), thermal chambers, ultra-high frequency sound waves, microwave, and laser [7].

Heat transport through biological tissues, represented by bioheat models, involves thermal conduction in tissue and vascular system, blood-tissue convection, and perfusion (through capillary tubes within the tissues) and also metabolic heat generation. Assuming local thermal equilibrium between the blood and the tissue, Pennes [10] represented one of the early and simplified bioheat equations. This model has been further developed by others such as Charny [11], Wulff [12], Klinger [13], Chen and Holmes [14], Weinbaum et al. [15–17], Mitchell and Myers [18], Keller and Seilder [19], Chen and Xu [20], Baish et al. [21,22], and Abraham and Sparrow [23]. Description of the established bioheat transport models can be found in the literature [11,24–26].

Advantages of utilizing porous media theory in modeling bioheat transfer, due to fewer assumptions as compared with different established bioheat transfer models, are stressed by Khanafer and Vafai [26], Nakayama and Kuwahara [27], Khaled and Vafai [28], and Mahjoob and Vafai [7]. The biological structure can be treated as a blood saturated porous matrix including cells and interstices, the so-called tissue. Utilizing the porous media theory, nonthermal equilibrium between the blood and the tissue is addressed and the blood-tissue convective heat exchange is taken into account. Volume averaging over each of the blood and tissue phases results in an energy equation for each individual phase [29–37,7], known as the local thermal nonequilibrium model. The volume averaging

[1]Corresponding author.
Contributed by the Heat Transfer Division of ASME for publication in the JOURNAL OF HEAT TRANSFER. Manuscript received June 10, 2009; final manuscript received August 12, 2009; published online December 30, 2009. Editor: Yogesh Jaluria.

over a representative elementary volume containing both the blood and tissue phases results in a local thermal equilibrium model referred to as the one equation model.

One of the shortcomings in most bioheat studies is modeling the target tissue/organ as a single tissue/organ with the same tissue properties. This type of modeling may not predict precisely heat transport through tissue layers in which there is a considerable variation in properties of the adjacent layers. As such, there would be a need to develop and utilize bioheat model for a dual layer. Dual layer bioheat modeling is also important relative to skin bioheat transport and burn injuries [38,39]. In addition, in hyperthermia treatment, utilizing a two layer model (consisting of cancerous and normal tissue layers) gives a more accurate prediction of temperature profile and heat transport through these layers [40].

Due to the importance of accurate prediction of temperature profile in tissues/organs in thermal therapies such as hyperthermia, heat transport through multilayer biological tissues has been investigated in this work. Mahjoob and Vafai [7] previously developed, for the first time, comprehensive analytical solutions for tissue and blood temperature profiles and heat transfer correlations for a single layer tissue subject to an imposed heat flux. In this work, bioheat transport through dual layer tissues subject to an imposed heat flux is investigated comprehensively. Precise correlations are obtained for the first time for a two layer media, which can be extended to a multilayer media.

Utilizing the local thermal nonequilibrium model of porous media theory, exact solutions for the tissue and blood temperature distributions in each layer are established, for the first time, for two primary tissue/organ models representing isolated and uniform temperature conditions. Each layer can have its own properties independent of the other layer. These exact solutions can be utilized for different types of tissues and organs considering each layer's effective parameters such as the vascular volume fraction, tissue matrix permeability and size, blood pressure and velocity, metabolic heat generation, and also imposed heat flux and body core temperature. As a result, the current models for temperature prediction during thermal therapies can be modified to present a more accurate temperature distribution within healthy and diseased cells.

2 Modeling and Formulation

2.1 Problem Description. Biological media usually consist of blood vessels, cells, and interstitial space, which can be categorized as vascular and extravascular regions (Fig. 1(*a*)). As such, a biological structure can be modeled as a porous matrix, including cells and interstitial space, called tissue, in which the blood infiltrates through. In this work, a dual layer, which can be expanded to a multilayer, biological media subject to an imposed heat flux, as in hyperthermia, while incorporating blood and tissue local heat exchange, is investigated. The blood and tissue temperature profiles in each layer are established analytically, incorporating the effects of the imposed heat flux, blood and tissue physical properties, arterial blood velocity, volume fraction of the vascular space and geometrical properties of the biological structure, internal heat generation within the tissue (e.g., metabolic heat generation) at each layer, and the heat penetration depth. The analysis is performed for two primary conditions, namely, isolated core region and uniform core temperature conditions. For the first model, a thermally isolated boundary condition exists at a depth of (D_1+D_2) from the surface of the tissue, where D_1 is the thickness of the layer exposed to the heat flux and D_2 is the thickness of the adjacent layer. This model is also applicable as a symmetry thermal boundary condition, in which the heat flux is imposed from both sides of the organ (Fig. 1(*b*)). The second primary model is based on the physical representation of the core tissue/organ at a prescribed temperature value at depth (D_1+D_2) through imposition of a uniform temperature at that depth. Flow is considered to be hydraulically and thermally developed. Natural convection and radiation are assumed to be negligible and thermodynamic properties of the tissue and blood are considered to be temperature independent over the range of temperature variations considered in bioheat transport applications.

2.2 Physical Description of Governing Equations and Boundary Conditions. The anatomic structure is modeled as a porous medium consisting of the blood and the tissue (solid matrix) phases. The governing energy equations for the blood and tissue phases incorporating internal heat sources (e.g., metabolic reactions) and local thermal nonequilibrium conditions, developed based on the theory of porous media [26–37], are represented in Ref. [7]. The imposed heat flux at the organ's surface can be represented under the local thermal nonequilibrium conditions, in which the flux is divided between the two tissue and blood phases based on their effective thermal conductivity and temperature gradient. The temperature at the tissue/organ surface subject to imposed heat flux is likely to be uniform and the same as those of the tissue solid matrix and the blood adjacent the organ surface [7,33,36,37].

The external heat flux influences the tissue within a depth of D_1+D_2. As discussed earlier, two primary models are investigated for the boundary condition at the depth of D_1+D_2 from the surface, which is subject to a given heat flux. These are the (i) isolated core region and (ii) uniform core temperature (T_c) at a depth (D_1+D_2), as shown in Fig. 1. The value of the uniform temperature (T_c) can be assigned as the body core temperature or a safe temperature so as not to damage the healthy tissues. At the interface of the layers, the continuity of temperature and flux is valid. The tissue and blood temperatures at the interface of the layers $(T_{t,i}$ and $T_{b,i})$ should be evaluated by solving the governing equations in each layer and applying the boundary conditions.

2.3 Normalization. The governing equations are normalized by utilizing the following nondimensional variables (j is a layer indicator, which is either 1 or 2 for the first or second tissue layer, respectively):

$$\eta = \frac{y}{D_1}, \quad \theta_{b,j} = \frac{k_{t,\mathrm{eff},1}(\langle T_{b,j}\rangle^b - T_s)}{q_s D_1}, \quad \theta_{t,j} = \frac{k_{t,\mathrm{eff},1}(\langle T_{t,j}\rangle^t - T_s)}{q_s D_1}$$

$$\Phi_j = \frac{(1-\varepsilon_j)D_1 \dot{q}_{\mathrm{gen},j}}{q_s}, \quad \mathrm{Bi}_j = \frac{h_{tb,j} a_{tb,j} D_1^2}{k_{t,\mathrm{eff},1}}, \quad \kappa = \frac{k_{b,\mathrm{eff},1}}{k_{t,\mathrm{eff},1}} \tag{1}$$

$$\xi_t = \frac{k_{t,\mathrm{eff},2}}{k_{t,\mathrm{eff},1}}, \quad \xi_b = \frac{k_{b,\mathrm{eff},2}}{k_{t,\mathrm{eff},1}}, \quad D = \frac{D_1}{D_2}$$

where parameters $\langle T_b\rangle^b$, $\langle T_t\rangle^t$, $k_{b,\mathrm{eff}}$, $k_{t,\mathrm{eff}}$, and ε represent the intrinsic phase average blood and tissue temperatures, blood and tissue effective thermal conductivities, and porosity (the volume fraction of the vascular space), respectively. The blood-tissue interfacial heat transfer coefficient is represented by h_{tb} and the specific surface area by a_{tb}, and $\dot{q}_{\mathrm{gen}}$ is the heat generation within the biological tissue (e.g., metabolic heat generation) [7]. The Biot number Bi in this case represents the ratio of the conduction resistance within the tissue matrix to the thermal resistance associated with the internal convective heat exchange between the tissue matrix and the blood phase.

2.4 Governing Equations and Boundary Conditions. Biological tissues differ from each other in both their porous features and compositions. Therapeutic approaches can be optimized through understanding a range of phenomena including the response of tissues under different physiological conditions. Tissue usually consists of blood vessels, cells, and interstitial space, which can be, categorized as vascular and extravascular regions. The properties of tissues can be approximated based on the assumption that it is a homogeneous porous medium. Direct measurement of the properties of tissues is difficult. Efforts have been devoted to the characterization of the pertinent parameters. The

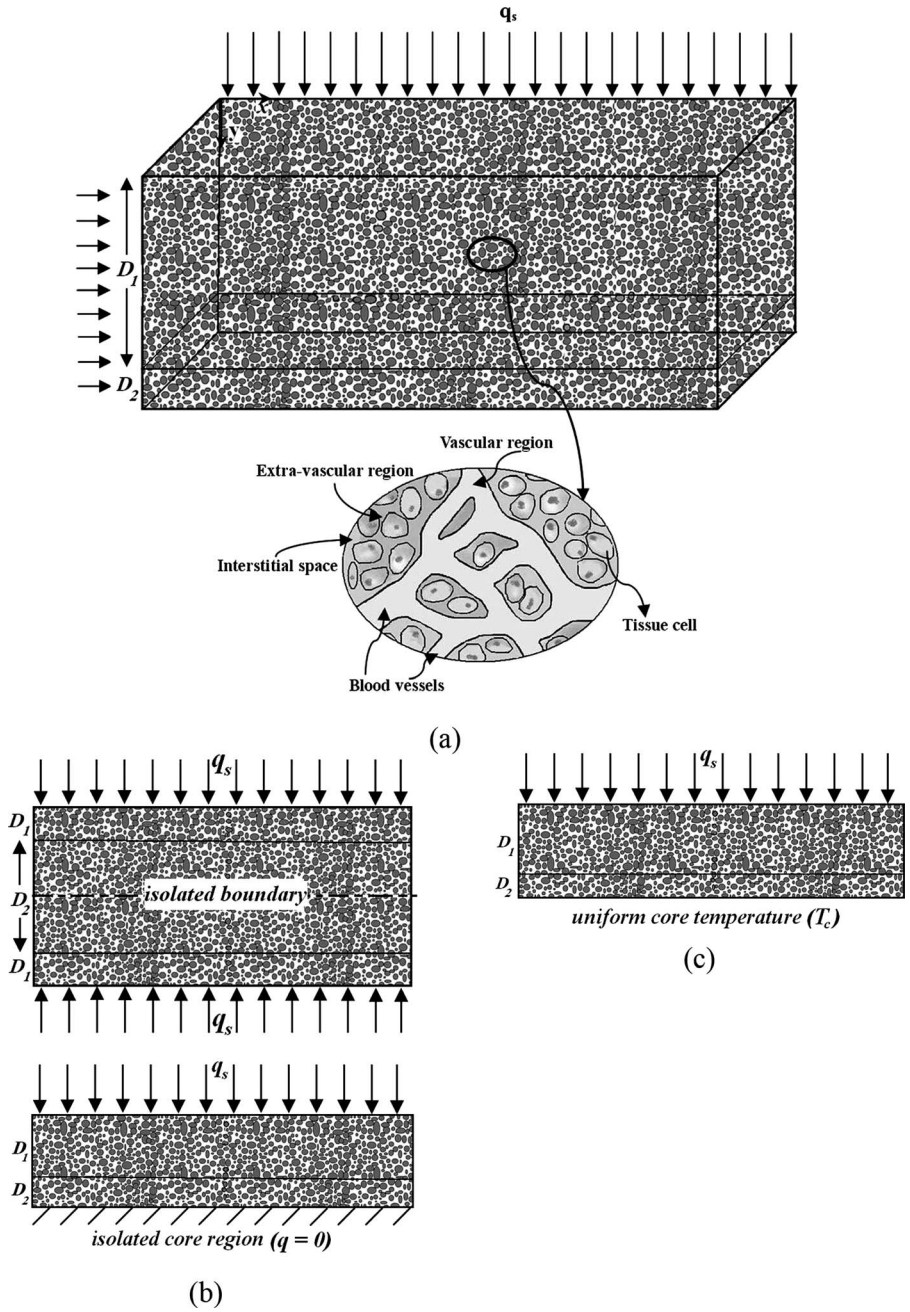

Fig. 1 Schematic diagram of (*a*) the multilayer tissue-vascular system, (*b*) model I (peripheral heat flux or isolated core region), and (*c*) model II (uniform core temperature)

obtained analytical expressions offer a versatile approach by allowing incorporation of variations in the representative volume fraction as well as various physical attributes. Some prior investigations have been performed based on the assumption that the arterial wall layers/tissues are porous structures with physical properties, which can be identified using the pore theory described by Khakpour and Vafai [41]. The properties for various layers can be based upon appropriate pore theory [41,42], fiber matrix models [42–47], and in vivo and in vitro experiments. The governing equations given by Mahjoob and Vafai [7] can be casted as follows:

First layer (with an imposed heat flux at the top):

$$\kappa\frac{\partial^4\theta_{b,1}}{\partial\eta^4} - \mathrm{Bi}_1(1+k)\left(\frac{\partial^2\theta_{b,1}}{\partial\eta^2}\right) = \Lambda \tag{2}$$

$$\kappa\frac{\partial^4\theta_{t,1}}{\partial\eta^4} - \mathrm{Bi}_1(1+k)\left(\frac{\partial^2\theta_{t,1}}{\partial\eta^2}\right) = \Lambda \tag{3}$$

Second layer (with an isolated or uniform temperature region at the bottom):

$$\xi_b\frac{\partial^4\theta_{b,2}}{\partial\eta^4} - \mathrm{Bi}_2\left(1+\frac{\xi_b}{\xi_t}\right)\frac{\partial^2\theta_{b,2}}{\partial\eta^2} = \Lambda' \tag{4}$$

$$\xi_b\frac{\partial^4\theta_{t,2}}{\partial\eta^4} - \mathrm{Bi}_2\left(1+\frac{\xi_b}{\xi_t}\right)\frac{\partial^2\theta_{t,2}}{\partial\eta^2} = \Lambda' \tag{5}$$

where in model I (isolated core region)

$$\Lambda = -\mathrm{Bi}_1(1+\kappa f_1 + g_1) \tag{6}$$

$$\Lambda' = \frac{D\mathrm{Bi}_2}{\xi_t}(\kappa f_1 + g_1) \tag{7}$$

and in model II (uniform core temperature)

$$\Lambda = -\mathrm{Bi}_1(1 + \kappa\theta_{b,i} + \theta_{t,i}) \tag{8}$$

$$\Lambda' = \mathrm{Bi}_2\left\{-D^2\left(1 + \frac{\xi_b}{\xi_t}\right)\theta_c + \frac{D(D\xi_b + \kappa)}{\xi_t}\theta_{b,i} + \frac{D(D\xi_t + 1)}{\xi_t}\theta_{t,i}\right\} \tag{9}$$

and

$$f_1 = \left.\frac{\partial\theta_{b,1}}{\partial\eta}\right|_{\eta=1} \tag{10}$$

$$g_1 = \left.\frac{\partial\theta_{t,1}}{\partial\eta}\right|_{\eta=1} \tag{11}$$

$$\theta_c = \frac{k_{t,\mathrm{eff},1}(T_c - T_s)}{q_s D_1} \tag{12}$$

$$\theta_{b,i} = \frac{k_{t,\mathrm{eff},1}(T_{b,i} - T_s)}{q_s D_1} \tag{13}$$

$$\theta_{t,i} = \frac{k_{t,\mathrm{eff},1}(T_{t,i} - T_s)}{q_s D_1} \tag{14}$$

Furthermore, the normalized boundary conditions are presented for each model as follows. Additional boundary conditions to solve the obtained fourth order blood/tissue energy equations (Eqs. (2)–(9)) can be obtained by evaluating the second or third order derivatives of θ_b and θ_t at the boundaries. This results in the following set of boundary conditions for each model:

Boundary conditions:

$$\theta_{b,1}|_{\eta=0} = \theta_{t,1}|_{\eta=0} = 0 \tag{15}$$

$$\theta_{b,1}|_{\eta=1} = \theta_{b,2}|_{\eta=1} = \theta_{b,i} \tag{16}$$

$$\theta_{t,1}|_{\eta=1} = \theta_{t,2}|_{\eta=1} = \theta_{t,i} \tag{17}$$

$$\left.\frac{\partial^2\theta_{t,1}}{\partial\eta^2}\right|_{\eta=0} = -\Phi_1 \tag{18}$$

$$\left.\frac{\partial^2\theta_{t,1}}{\partial\eta^2}\right|_{\eta=1} = -\Phi_1 + \mathrm{Bi}_1(\theta_{t,i} - \theta_{b,i}) \tag{19}$$

$$\left.\frac{\partial^2\theta_{t,2}}{\partial\eta^2}\right|_{\eta=1} = \frac{-1}{\xi_t}(\Phi_2 + \mathrm{Bi}_2(\theta_{b,i} - \theta_{t,i})) \tag{20}$$

$$\kappa\left.\frac{\partial\theta_{b,1}}{\partial\eta}\right|_{\eta=1} + \left.\frac{\partial\theta_{t,1}}{\partial\eta}\right|_{\eta=1} = \xi_b\left.\frac{\partial\theta_{b,2}}{\partial\eta}\right|_{\eta=1} + \xi_t\left.\frac{\partial\theta_{t,2}}{\partial\eta}\right|_{\eta=1} \tag{21}$$

The other normalized boundary conditions for the two primary models are as follows:

For model I (isolated core region):

$$\left.\frac{\partial^2\theta_{b,1}}{\partial\eta^2}\right|_{\eta=0} = \frac{1}{\kappa}(1 + \Phi_1 + \kappa f_1 + g_1) \tag{22}$$

$$\left.\frac{\partial^2\theta_{b,1}}{\partial\eta^2}\right|_{\eta=1} = \frac{1}{\kappa}(1 + \Phi_1 + \kappa f_1 + g_1 + \mathrm{Bi}_1(\theta_{b,i} - \theta_{t,i})) \tag{23}$$

$$\left.\frac{\partial^2\theta_{b,2}}{\partial\eta^2}\right|_{\eta=1} = \frac{1}{\xi_b}(-D(\kappa f_1 + g_1) + \Phi_2 + \mathrm{Bi}_2(\theta_{b,i} - \theta_{t,i})) \tag{24}$$

$$\left.\frac{\partial\theta_{b,2}}{\partial\eta}\right|_{\eta=1+1/D} = \left.\frac{\partial\theta_{t,2}}{\partial\eta}\right|_{\eta=1+1/D} = 0 \tag{25}$$

$$\left.\frac{\partial^3\theta_{b,2}}{\partial\eta^3}\right|_{\eta=1+1/D} = \left.\frac{\partial^3\theta_{t,2}}{\partial\eta^3}\right|_{\eta=1+1/D} = 0 \tag{26}$$

and for model II (uniform core temperature):

$$\left.\frac{\partial^2\theta_{b,1}}{\partial\eta^2}\right|_{\eta=0} = \frac{1}{\kappa}(1 + \Phi_1 + \kappa\theta_{b,i} + \theta_{t,i}) \tag{27}$$

$$\left.\frac{\partial^2\theta_{b,1}}{\partial\eta^2}\right|_{\eta=1} = \frac{1}{\kappa}(1 + \Phi_1 + (\kappa + \mathrm{Bi}_1)\theta_{b,i} + (1 - \mathrm{Bi}_1)\theta_{t,i}) \tag{28}$$

$$\left.\frac{\partial^2\theta_{b,2}}{\partial\eta^2}\right|_{\eta=1} = \frac{1}{\xi_b}[\{\mathrm{Bi}_2 - D(D\xi_b + \kappa)\}\theta_{b,i} - \{\mathrm{Bi}_2 + D(D\xi_t + 1)\}\theta_{t,i} + \Phi_2] + D^2\left(1 + \frac{\xi_t}{\xi_b}\right)\theta_c \tag{29}$$

$$\theta_{b,2}|_{\eta=1+1/D} = \theta_{t,2}|_{\eta=1+1/D} = \theta_c \tag{30}$$

$$\left.\frac{\partial^2\theta_{b,2}}{\partial\eta^2}\right|_{\eta=1+1/D} = -D\left(D + \frac{\kappa}{\xi_b}\right)\theta_{b,i} - \frac{D}{\xi_b}(D\xi_t + 1)\theta_{t,i} + D^2\left(1 + \frac{\xi_t}{\xi_b}\right)\theta_c + \frac{\Phi_2}{\xi_b} \tag{31}$$

$$\left.\frac{\partial^2\theta_{t,2}}{\partial\eta^2}\right|_{\eta=1+1/D} = -\frac{\Phi_2}{\xi_t} \tag{32}$$

2.5 Blood, Tissue, and Surface Temperature Fields. Blood and tissue phase temperature distributions can be obtained by solving the governing equations and utilizing the Neumann and Dirichlet boundary conditions. After a lengthy analysis, the blood and tissue temperature profiles are obtained as follows (for brevity, the volume averaging sign ($\langle\ \rangle$) is dropped).

2.5.1 Model I: Isolated Core Region

2.5.1.1 First layer.

$$\theta_{b,1} = \frac{1}{1+\kappa}\left(\frac{\eta}{2}\{(1 + \kappa f_1 + g_1)\eta - [1 - 2\kappa\theta_{b,i} - 2\theta_{t,i} + \kappa f_1 + g_1]\} - \frac{1 + (1+\kappa)\Phi_1 + \kappa f_1 + g_1}{(1+\kappa)\mathrm{Bi}_1}\left\{1 - \frac{e^{\lambda\eta} + e^{\lambda(1-\eta)}}{1 + e^{\lambda}}\right\} + (\theta_{b,i} - \theta_{t,i})\frac{e^{\lambda(1+\eta)} - e^{\lambda(1-\eta)}}{e^{2\lambda} - 1}\right) \tag{33}$$

$$\theta_{t,1} = \frac{1}{1+\kappa}\left(\frac{\eta}{2}\{(1 + \kappa f_1 + g_1)\eta - [1 - 2\kappa\theta_{b,i} - 2\theta_{t,i} + \kappa f_1 + g_1]\} + \frac{\kappa[1 + (1+\kappa)\Phi_1 + \kappa f_1 + g_1]}{(1+\kappa)\mathrm{Bi}_1}\left\{1 - \frac{e^{\lambda\eta} + e^{\lambda(1-\eta)}}{1 + e^{\lambda}}\right\} - \kappa(\theta_{b,i} - \theta_{t,i})\frac{e^{\lambda(1+\eta)} - e^{\lambda(1-\eta)}}{e^{2\lambda} - 1}\right) \tag{34}$$

where

$$\lambda = \sqrt{\mathrm{Bi}_1(1+\kappa)/\kappa} \tag{35}$$

The blood $\theta_{b,i}$ and tissue $\theta_{t,i}$ temperatures at the interface would be evaluated after obtaining their corresponding temperature profiles in the second layer. Terms f_1 and g_1 can be evaluated based on their definition (Eqs. (10) and (11)) and the obtained blood and tissue temperature profiles in the first layer. This results in

$$f_1 = \frac{1}{1+\kappa}\left(\frac{\{2+(1+\kappa)\Phi_1+2\kappa\theta_{b,i}+2\theta_{t,i}\}(e^{\lambda}-1)}{\lambda\kappa(1+e^{\lambda})} + \lambda(\theta_{b,i}-\theta_{t,i})\frac{e^{2\lambda}+1}{e^{2\lambda}-1}+1+2\kappa\theta_{b,i}+2\theta_{t,i}\right) \quad (36)$$

$$g_1 = \frac{-1}{1+\kappa}\left(\frac{\{2+(1+\kappa)\Phi_1+2\kappa\theta_{b,i}+2\theta_{t,i}\}(e^{\lambda}-1)}{\lambda(1+e^{\lambda})} + \lambda\kappa(\theta_{b,i}-\theta_{t,i})\frac{e^{2\lambda}+1}{e^{2\lambda}-1}-1-2\kappa\theta_{b,i}-2\theta_{t,i}\right) \quad (37)$$

Substituting f_1 and g_1 in Eqs. (33) and (34) gives

$$\theta_{b,1} = \frac{1}{1+\kappa}\left(\eta\{(1+\kappa\theta_{b,i}+\theta_{t,i})\eta-1\}+(\theta_{b,i}-\theta_{t,i})\frac{e^{\lambda(1+\eta)}-e^{\lambda(1-\eta)}}{e^{2\lambda}-1} - \frac{2(1+\kappa\theta_{b,i}+\theta_{t,i})+(1+\kappa)\Phi_1}{(1+\kappa)\mathrm{Bi}_1}\left\{1-\frac{e^{\lambda\eta}+e^{\lambda(1-\eta)}}{1+e^{\lambda}}\right\}\right) \quad (38)$$

$$\theta_{t,1} = \frac{1}{1+\kappa}\left(\eta\{(1+\kappa\theta_{b,i}+\theta_{t,i})\eta-1\}-\kappa(\theta_{b,i}-\theta_{t,i})\frac{e^{\lambda(1+\eta)}-e^{\lambda(1-\eta)}}{e^{2\lambda}-1}+\frac{\kappa[2(1+\kappa\theta_{b,i}+\theta_{t,i})+(1+\kappa)\Phi_1]}{(1+\kappa)\mathrm{Bi}_1} \times\left\{1-\frac{e^{\lambda\eta}+e^{\lambda(1-\eta)}}{1+e^{\lambda}}\right\}\right) \quad (39)$$

As such, the temperature difference between the tissue and blood phases and the blood mean temperature can be written as

$$\Delta\theta_1 = \theta_{t,1}-\theta_{b,1} = (\theta_{b,i}-\theta_{t,i})\frac{e^{\lambda(1-\eta)}-e^{\lambda(1+\eta)}}{e^{2\lambda}-1} + \frac{2(1+\kappa\theta_{b,i}+\theta_{t,i})+(1+\kappa)\Phi_1}{(1+\kappa)\mathrm{Bi}_1}\left\{1-\frac{e^{\lambda\eta}+e^{\lambda(1-\eta)}}{1+e^{\lambda}}\right\} \quad (40)$$

$$\theta_{b,1,m} = \left(\frac{2[2+2\kappa\theta_{b,i}+2\theta_{t,i}+(1+\kappa)\Phi_1]}{\lambda^3\kappa(1+\kappa)}+\frac{\theta_{b,i}-\theta_{t,i}}{\lambda(1+\kappa)}\right)\left(\frac{e^{\lambda}-1}{e^{\lambda}+1}\right) + \frac{-1+2\kappa\theta_{b,i}+2\theta_{t,i}}{6(1+\kappa)}-\frac{1}{\lambda^2\kappa(1+\kappa)} \times\{2+2\kappa\theta_{b,i}+2\theta_{t,i}+(1+\kappa)\Phi_1\} \quad (41)$$

2.5.1.2 Second layer.

$$\theta_{b,2} = \frac{1}{(\xi_b+\xi_t)}\left((1+2\kappa\theta_{b,i}+2\theta_{t,i})\left\{\left(\frac{-D}{2}\eta+D+1\right)\eta-1-\frac{D}{2}+\frac{D\xi_t^2}{\mathrm{Bi}_2(\xi_b+\xi_t)}\right\}+\xi_t\left(\theta_{b,i}-\theta_{t,i}+\frac{\Phi_2}{\mathrm{Bi}_2} - \frac{D\xi_t(1+2\kappa\theta_{b,i}+2\theta_{t,i})}{\mathrm{Bi}_2(\xi_b+\xi_t)}\right)\left(\frac{e^{\lambda'(\eta-1)}+e^{\lambda'(1+(2/D)-\eta)}}{e^{2\lambda'/D}+1}\right) + \xi_b\theta_{b,i}+\xi_t\theta_{t,i}-\frac{\xi_t\Phi_2}{\mathrm{Bi}_2}\right) \quad (42)$$

$$\theta_{t,2} = \frac{1}{(\xi_b+\xi_t)}\left((1+2\kappa\theta_{b,i}+2\theta_{t,i})\left\{\left(\frac{-D}{2}\eta+D+1\right)\eta-1-D/2-\frac{D\xi_b\xi_t}{\mathrm{Bi}_2(\xi_b+\xi_t)}\right\}-\xi_b\left(\theta_{b,i}-\theta_{t,i}+\frac{\Phi_2}{\mathrm{Bi}_2} - \frac{D\xi_t(1+2\kappa\theta_{b,i}+2\theta_{t,i})}{\mathrm{Bi}_2(\xi_b+\xi_t)}\right)\left(\frac{e^{\lambda'(\eta-1)}+e^{\lambda'(1+(2/D)-\eta)}}{e^{2\lambda'/D}+1}\right) + \xi_b\theta_{b,i}+\xi_t\theta_{t,i}+\frac{\xi_b\Phi_2}{\mathrm{Bi}_2}\right) \quad (43)$$

where

$$\lambda' = \sqrt{\frac{\xi_b+\xi_t}{\xi_b\xi_t}\mathrm{Bi}_2} \quad (44)$$

Based on the above results, the temperature difference between the tissue and blood phases for the second layer is obtained as

$$\Delta\theta_2 = \theta_{t,2}-\theta_{b,2} = -\left(\theta_{b,i}-\theta_{t,i}+\frac{\Phi_2}{\mathrm{Bi}_2}-\frac{D\xi_t(1+2\kappa\theta_{b,i}+2\theta_{t,i})}{\mathrm{Bi}_2(\xi_b+\xi_t)}\right) \times\left(\frac{e^{\lambda'(\eta-1)}+e^{\lambda'(1+(2/D)-\eta)}}{e^{2\lambda'/D}+1}\right)-\frac{D\xi_t(1+2\kappa\theta_{b,i}+2\theta_{t,i})}{\mathrm{Bi}_2(\xi_b+\xi_t)}+\frac{\Phi_2}{\mathrm{Bi}_2} \quad (45)$$

Finally, the mean blood temperature for the second layer can be written as

$$\theta_{b,2,m} = D\xi_t\left(\frac{\mathrm{Bi}_2(\xi_b+\xi_t)(\theta_{b,i}-\theta_{t,i})-D\xi_t(1+2\kappa\theta_{b,i}+2\theta_{t,i})+(\xi_b+\xi_t)\Phi_2}{\lambda'\mathrm{Bi}_2(\xi_b+\xi_t)^2}\right)\frac{e^{2\lambda'/D}-1}{e^{2\lambda'/D}+1}+(1+2\kappa\theta_{b,i}+2\theta_{t,i})\left\{\frac{1}{3D(\xi_b+\xi_t)}+\frac{D\xi_t^2}{\mathrm{Bi}_2(\xi_b+\xi_t)^2}\right\} + \frac{\xi_b\theta_{b,i}+\xi_t\theta_{t,i}}{\xi_b+\xi_t}-\frac{\xi_t\Phi_2}{\mathrm{Bi}_2(\xi_b+\xi_t)} \quad (46)$$

2.5.1.3 Interface blood and tissue temperatures. To evaluate the blood and tissue temperatures at the interface of the layers ($\theta_{b,i}$ and $\theta_{t,i}$), two equations are required. One of these equations is obtained based on the fully developed temperature profile subject to a uniform heat flux on one side and an insulated condition on the other side. This results in

$$1+2\kappa\theta_{b,i}+2\theta_{t,i} = \frac{(\rho c_p u_a)_1 D_1 D_2(1-\varepsilon_2)\dot{q}_{\mathrm{gen},2}-(\rho c_p u_a)_2 D_2(q_s+D_1(1-\varepsilon_1)\dot{q}_{\mathrm{gen},1})}{q_s[(\rho c_p u_a)_2 D_2+(\rho c_p u_a)_1 D_1]} \quad (47)$$

The other equation is obtained by utilizing the derived analytical solution for a single layer [7]. The temperature profiles for the blood and tissue phases in a double layer (present work) are taken to be the same as those in a single layer [7], within the distance of D_1 from the surface subject to an imposed heat flux. Rewriting the developed equations for a single layer [7] in the present coordinate system ($0 \le \eta \le 1+(1/D)$) gives

$$\theta_{t,i} - \theta_{b,i} = \frac{\dfrac{D_1}{(D_1+D_2)} + (1+\kappa)\Phi_1}{(1+\kappa)\mathrm{Bi}_1}\left(1 - \frac{e^{\lambda} + e^{\lambda(1+(2D_2/D_1))}}{1+e^{2\lambda(1+(D_2/D_1))}}\right) \tag{48}$$

The above two equations (Eqs. (59) and (60)) result in

$$\theta_{t,i} = \frac{1}{2(1+\kappa)}\left(\frac{(\rho c_p u_a)_1 D_1 D_2(1-\varepsilon_2)\dot{q}_{\mathrm{gen},2} - (\rho c_p u_a)_2 D_2(q_s + D_1(1-\varepsilon_1)\dot{q}_{\mathrm{gen},1})}{q_s[(\rho c_p u_a)_2 D_2 + (\rho c_p u_a)_1 D_1]} + 2\kappa\frac{D_1 + (1+\kappa)(D_1+D_2)\Phi_1}{(1+\kappa)(D_1+D_2)\mathrm{Bi}_1}\left(1 - \frac{e^{\lambda} + e^{\lambda(1+(2D_2/D_1))}}{1+e^{2\lambda(1+(D_2/D_1))}}\right) - 1\right) \tag{49}$$

$$\theta_{b,i} = \frac{1}{2(1+\kappa)}\left\{\frac{(\rho c_p u_a)_1 D_1 D_2(1-\varepsilon_2)\dot{q}_{\mathrm{gen},2} - (\rho c_p u_a)_2 D_2(q_s + D_1(1-\varepsilon_1)\dot{q}_{\mathrm{gen},1})}{q_s[(\rho c_p u_a)_2 D_2 + (\rho c_p u_a)_1 D_1]} - 1\right\} - \frac{D_1 + (1+\kappa)(D_1+D_2)\Phi_1}{(1+\kappa)^2(D_1+D_2)\mathrm{Bi}_1}\left(1 - \frac{e^{\lambda} + e^{\lambda(1+(2D_2/D_1))}}{1+e^{2\lambda(1+(D_2/D_1))}}\right) \tag{50}$$

The dimensional blood mean temperature and the body organ surface temperature, which is subject to an imposed heat flux, are derived to be

$$T_{b,1,m} = \frac{q_s + (1-\varepsilon_1)D_1\dot{q}_{\mathrm{gen},1} + D_2(1-\varepsilon_2)\dot{q}_{\mathrm{gen},2}}{(\rho c_p u_a)_2 D_2 + (\rho c_p u_a)_1 D_1}x + T_{a,1} \tag{51}$$

$$T_{b,2,m} = \frac{q_s + D_1(1-\varepsilon_1)\dot{q}_{\mathrm{gen},1} + (1-\varepsilon_2)D_2\dot{q}_{\mathrm{gen},2}}{(\rho c_p u_a)_2 D_2 + (\rho c_p u_a)_1 D_1}x + T_{a,2} \tag{52}$$

$$\begin{aligned} T_s = &-\frac{q_s D_1}{k_{t,\mathrm{eff},1}}\left(\left(\frac{4(e^{\lambda}-1)}{\lambda^3\kappa(e^{\lambda}+1)} + \frac{1}{3} - \frac{2}{\lambda^2\kappa}\right)\frac{(\rho c_p u_a)_1 D_1(-q_s + D_2(1-\varepsilon_2)\dot{q}_{\mathrm{gen},2}) - (\rho c_p u_a)_2 D_2(2q_s + D_1(1-\varepsilon_1)\dot{q}_{\mathrm{gen},1})}{2q_s(1+\kappa)[(\rho c_p u_a)_2 D_2 + (\rho c_p u_a)_1 D_1]}\right. \\ &\left. + \left(\frac{2[2+(1+\kappa)\Phi_1]}{\lambda^3\kappa(1+\kappa)} - \frac{D_1 + (1+\kappa)(D_1+D_2)\Phi_1}{\lambda(1+\kappa)^2(D_1+D_2)\mathrm{Bi}_1}\left(1 - \frac{e^{\lambda} + e^{\lambda(1+(2D_2/D_1))}}{1+e^{2\lambda(1+(D_2/D_1))}}\right)\right)\left(\frac{e^{\lambda}-1}{e^{\lambda}+1}\right) - \frac{1}{6(1+\kappa)} - \frac{2+(1+\kappa)\Phi_1}{\lambda^2\kappa(1+\kappa)}\right) \\ &+ \frac{q_s + (1-\varepsilon_1)D_1\dot{q}_{\mathrm{gen},1} + D_2(1-\varepsilon_2)q_{\mathrm{gen},2}}{(\rho c_p u_a)_2 D_2 + (\rho c_p u_a)_1 D_1}x + T_{a,1} \end{aligned} \tag{53}$$

The Nusselt number can be represented as

$$\mathrm{Nu}_s = \frac{h_s D_h}{k_{b,\mathrm{eff},1}} = \frac{-2}{\kappa\theta_{b,1,m}}\left(1 + \frac{1}{D}\right) = \frac{\dfrac{-2}{\kappa}\left(1+\dfrac{1}{D}\right)}{\left(\left(\dfrac{2[2+2\kappa\theta_{b,i}+2\theta_{t,i}+(1+\kappa)\Phi_1]}{\lambda^3\kappa(1+\kappa)} + \dfrac{\theta_{b,i}-\theta_{t,i}}{\lambda(1+\kappa)}\right)\left(\dfrac{e^{\lambda}-1}{e^{\lambda}+1}\right) + \dfrac{-1+2\kappa\theta_{b,i}+2\theta_{t,i}}{6(1+\kappa)} - \dfrac{1}{\lambda^2\kappa(1+\kappa)}(2+2\kappa\theta_{b,i}+2\theta_{t,i}+(1+\kappa)\Phi_1)\right)} \tag{54}$$

2.5.2 Model II: Uniform Core Temperature

2.5.2.1 First layer.

$$\theta_{b,1} = \frac{1}{(1+\kappa)}\left(\frac{\kappa\theta_{b,i}+\theta_{t,i}+1}{2}\eta^2 + \frac{\kappa\theta_{b,i}+\theta_{t,i}-1}{2}\eta - \frac{1}{\mathrm{Bi}_1}\left(\frac{\kappa\theta_{b,i}+\theta_{t,i}+1}{1+\kappa} + \Phi_1\right)\left\{1 - \frac{(e^{\lambda\eta}+e^{\lambda(1-\eta)})}{(1+e^{\lambda})}\right\} + (\theta_{b,i}-\theta_{t,i})\frac{e^{\lambda(1+\eta)} - e^{\lambda(1-\eta)}}{e^{2\lambda}-1}\right) \tag{55}$$

$$\theta_{t,1} = \frac{1}{(1+\kappa)}\left(\frac{\kappa\theta_{b,i}+\theta_{t,i}+1}{2}\eta^2 + \frac{\kappa\theta_{b,i}+\theta_{t,i}-1}{2}\eta + \frac{\kappa}{\mathrm{Bi}_1}\left(\frac{\kappa\theta_{b,i}+\theta_{t,i}+1}{1+\kappa} + \Phi_1\right)\left\{1 - \frac{(e^{\lambda\eta}+e^{\lambda(1-\eta)})}{(1+e^{\lambda})}\right\} - \kappa(\theta_{b,i}-\theta_{t,i})\frac{e^{\lambda(1+\eta)} - e^{\lambda(1-\eta)}}{e^{2\lambda}-1}\right) \tag{56}$$

where

$$\lambda = \sqrt{\mathrm{Bi}_1(1+\kappa)/\kappa} \tag{57}$$

and

$$\Delta\theta_1 = \theta_{t,1} - \theta_{b,1} = \frac{1}{\mathrm{Bi}_1}\left(\frac{\kappa\theta_{b,i} + \theta_{t,i} + 1}{1+\kappa} + \Phi_1\right)\left\{1 - \frac{(e^{\lambda\eta} + e^{\lambda(1-\eta)})}{(1+e^{\lambda})}\right\} - (\theta_{b,i} - \theta_{t,i})\frac{e^{\lambda(1+\eta)} - e^{\lambda(1-\eta)}}{e^{2\lambda} - 1} \tag{58}$$

$$\theta_{b,1,m} = \frac{1}{(1+\kappa)}\left((\kappa\theta_{b,i} + \theta_{t,i} + 1)\left(\frac{5}{12} - \frac{1}{\mathrm{Bi}_1(1+\kappa)}\left\{1 - \frac{2(e^{\lambda}-1)}{\lambda(1+e^{\lambda})}\right\}\right) - \frac{\Phi_1}{\mathrm{Bi}_1}\left\{1 - \frac{2(e^{\lambda}-1)}{\lambda(1+e^{\lambda})}\right\} + \frac{(\theta_{b,i} - \theta_{t,i})(e^{\lambda}-1)}{\lambda(1+e^{\lambda})} - \frac{1}{2}\right) \tag{59}$$

2.5.2.2 Second layer.

$$\begin{aligned}\theta_{b,2} = {} & \frac{A(e^{\lambda'(1+(2/D)-\eta)} - e^{\lambda'(\eta-1)}) + B(e^{\lambda'(1+(1/D)-\eta)} - e^{\lambda'((1/D)-1+\eta)})}{(e^{(2\lambda'/D)} - 1)} + \left(\frac{D^2}{2}\theta_c - \frac{D(D\xi_b+\kappa)}{2(\xi_b+\xi_t)}\theta_{b,i} - \frac{D(D\xi_t+1)}{2(\xi_b+\xi_t)}\theta_{t,i}\right)\eta^2 \\ & + \left\{D(0.5-D)\theta_c + \frac{\theta_{b,i}}{\xi_b+\xi_t}[-\xi_b D + (D+0.5)(D\xi_b+\kappa_1)] + \frac{\theta_{t,i}}{\xi_b+\xi_t}[-D\xi_t + (D+0.5)(D\xi_t+1)]\right\}\eta \\ & - \theta_c\left(\frac{D^2\xi_t^2}{\mathrm{Bi}_2(\xi_b+\xi_t)} + \frac{D}{2}(1-D)\right) + \frac{\theta_{b,i}}{\xi_b+\xi_t}\left(\begin{array}{l} -\dfrac{D\xi_b\xi_t(D\xi_b+\kappa)}{\mathrm{Bi}_2(\xi_b+\xi_t)} + \dfrac{D\xi_t(D\xi_b+\kappa)}{\mathrm{Bi}_2} + \\ \xi_b(1+D) - \dfrac{(1+D)}{2}(D\xi_b+\kappa)\end{array}\right) \\ & + \frac{\theta_{t,i}}{\xi_b+\xi_t}\left(-\frac{D\xi_b\xi_t(D\xi_t+1)}{\mathrm{Bi}_2(\xi_b+\xi_t)} + \frac{D\xi_t(D\xi_t+1)}{\mathrm{Bi}_2} - \frac{(1+D)}{2}(D\xi_t+1) + \xi_t(1+D)\right) - \frac{\xi_t\Phi_2}{\mathrm{Bi}_2(\xi_b+\xi_t)}\end{aligned} \tag{60}$$

$$\begin{aligned}\theta_{t,2} = {} & \frac{A'(e^{\lambda'(1+(2/D)-\eta)} - e^{\lambda'(\eta-1)}) + B'(e^{\lambda'(1+(1/D)-\eta)} - e^{\lambda'((1/D)-1+\eta)})}{(e^{(2\lambda'/D)} - 1)} + \left(\frac{D^2}{2}\theta_c - \frac{D(D\xi_b+\kappa)}{2(\xi_b+\xi_t)}\theta_{b,i} - \frac{D(D\xi_t+1)}{2(\xi_b+\xi_t)}\theta_{t,i}\right)\eta^2 \\ & + \left\{D(0.5-D)\theta_c + \frac{\theta_{b,i}}{\xi_b+\xi_t}[-\xi_b D + (D+0.5)(D\xi_b+\kappa_1)] + \frac{\theta_{t,i}}{\xi_b+\xi_t}[-D\xi_t + (D+0.5)(D\xi_t+1)]\right\}\eta + \theta_c\left(\frac{D^2\xi_b\xi_t}{\mathrm{Bi}_2(\xi_b+\xi_t)} + \frac{D}{2}(D-1)\right) \\ & - \frac{\theta_{b,i}}{\xi_b+\xi_t}\left(\begin{array}{l} \dfrac{D\xi_b\xi_t(D\xi_b+\kappa)}{\mathrm{Bi}_2(\xi_b+\xi_t)} + \dfrac{D(D\xi_b+\kappa)}{2} - \\ \xi_b(1+D) + \dfrac{D\xi_b+\kappa}{2}\end{array}\right) - \frac{\theta_{t,i}}{\xi_b+\xi_t}\left(\frac{D\xi_b\xi_t(D\xi_t+1)}{\mathrm{Bi}_2(\xi_b+\xi_t)} + \frac{D(D\xi_t+1)}{2} + \frac{D\xi_t+1}{2} - \xi_t(1+D)\right) + \frac{\xi_b\Phi_2}{\mathrm{Bi}_2(\xi_b+\xi_t)}\end{aligned} \tag{61}$$

$$\Delta\theta_2 = \theta_{t,2} - \theta_{b,2} = \frac{A''(e^{\lambda'(1+(2/D)-\eta)} - e^{\lambda'(\eta-1)}) + B''(e^{\lambda'(1+(1/D)-\eta)} - e^{\lambda'((1/D)-1+\eta)})}{(e^{(2\lambda'/D)} - 1)} + \frac{\xi_t D^2}{\mathrm{Bi}_2}\theta_c - \frac{D\xi_t(D\xi_b+\kappa)}{\mathrm{Bi}_2(\xi_b+\xi_t)}\theta_{b,i} - \frac{D\xi_t(D\xi_t+1)}{\mathrm{Bi}_2(\xi_b+\xi_t)}\theta_{t,i} + \frac{\Phi_2}{\mathrm{Bi}_2} \tag{62}$$

where

$$A = \frac{\xi_t}{\xi_b+\xi_t}\left\{\frac{\xi_t D^2}{\mathrm{Bi}_2}\theta_c + \left(1 - \frac{D\xi_t(D\xi_b+\kappa)}{\mathrm{Bi}_2(\xi_b+\xi_t)}\right)\theta_{b,i} - \left(1 + \frac{D\xi_t(D\xi_t+1)}{\mathrm{Bi}_2(\xi_b+\xi_t)}\right)\theta_{t,i} + \frac{\Phi_2}{\mathrm{Bi}_2}\right\} \tag{63}$$

$$B = \frac{\xi_t}{(\xi_b+\xi_t)\mathrm{Bi}_2}\left\{-\xi_t D^2\theta_c + \frac{D\xi_t(D\xi_b+\kappa)}{(\xi_b+\xi_t)}\theta_{b,i} + \frac{D\xi_t(D\xi_t+1)}{(\xi_b+\xi_t)}\theta_{t,i} - \Phi_2\right\} \tag{64}$$

$$A' = \frac{\xi_t}{\xi_b+\xi_t}\left\{-\frac{\xi_b D^2}{\mathrm{Bi}_2}\theta_c + \left(-\frac{\xi_b}{\xi_t} + \frac{D\xi_b(D\xi_b+\kappa)}{\mathrm{Bi}_2(\xi_b+\xi_t)}\right)\theta_{b,i} + \left(\frac{\xi_b}{\xi_t} + \frac{D\xi_b(D\xi_t+1)}{\mathrm{Bi}_2(\xi_b+\xi_t)}\right)\theta_{t,i} - \frac{\xi_b\Phi_2}{\mathrm{Bi}_2\xi_t}\right\} \tag{65}$$

$$B' = \frac{\xi_t}{\xi_b+\xi_t}\left\{\frac{\xi_b D^2}{\mathrm{Bi}_2}\theta_c - \frac{D\xi_b(D\xi_b+\kappa)}{\mathrm{Bi}_2(\xi_b+\xi_t)}\theta_{b,i} - \frac{D\xi_b(D\xi_t+1)}{\mathrm{Bi}_2(\xi_b+\xi_t)}\theta_{t,i} + \frac{\xi_b\Phi_2}{\mathrm{Bi}_2\xi_t}\right\} \tag{66}$$

$$A'' = -\frac{\xi_t D^2}{\mathrm{Bi}_2}\theta_c + \left(\frac{D\xi_t(D\xi_b+\kappa)}{\mathrm{Bi}_2(\xi_b+\xi_t)} - 1\right)\theta_{b,i} + \left(\frac{D\xi_t(D\xi_t+1)}{\mathrm{Bi}_2(\xi_b+\xi_t)} + 1\right)\theta_{t,i} - \frac{\Phi_2}{\mathrm{Bi}_2} \tag{67}$$

$$B'' = \frac{\xi_t D^2}{\mathrm{Bi}_2}\theta_c - \frac{D\xi_t(D\xi_b+\kappa)}{\mathrm{Bi}_2(\xi_b+\xi_t)}\theta_{b,i} - \frac{D\xi_t(D\xi_t+1)}{\mathrm{Bi}_2(\xi_b+\xi_t)}\theta_{t,i} + \frac{\Phi_2}{\mathrm{Bi}_2} \tag{68}$$

$$\lambda' = \sqrt{\frac{\xi_b+\xi_t}{\xi_b\xi_t}\mathrm{Bi}_2} \tag{69}$$

2.5.2.3 Interface blood and tissue temperatures. Blood and tissue temperatures at the interface of the layers ($\theta_{b,i}$ and $\theta_{t,i}$) can be evaluated by utilizing the boundary condition given by Eq. (21), the derived analytical solution for one layer hyperthermia for the equivalent case [7], and the derived profiles for blood and tissue in each layer. This results in

$$\theta_{t,i}=\frac{1}{2(1+\kappa)+D(\xi_b+\xi_t)}\left(\frac{(2\kappa+D\xi_b)\left\{(1+\kappa)\left[\theta_c+\Phi_1\left(1+\frac{1}{D}\right)^2\right]+\frac{1}{D}+1\right\}}{(1+\kappa)\mathrm{Bi}_1\left(1+\frac{1}{D}\right)^2}\left[1-\frac{e^{\lambda}+e^{\lambda/D}}{1+e^{\lambda(1+(1/D))}}\right]+D(\xi_b+\xi_t)\theta_c-1\right) \tag{70}$$

$$\theta_{b,i}=\frac{1}{2(1+\kappa)+D(\xi_b+\xi_t)}\left(-\frac{(2+D\xi_t)\left\{(1+\kappa)\left[\theta_c+\Phi_1\left(1+\frac{1}{D}\right)^2\right]+\frac{1}{D}+1\right\}}{(1+\kappa)\mathrm{Bi}_1\left(1+\frac{1}{D}\right)^2}\left[1-\frac{e^{\lambda}+e^{\lambda/D}}{1+e^{\lambda(1+(1/D))}}\right]+D(\xi_b+\xi_t)\theta_c-1\right) \tag{71}$$

The dimensional blood mean temperature, body organ surface temperature, and heat exchange rate represented by a Nusselt number at the body organ surface, which is subjected to an imposed heat flux, are derived to be

$$T_{b,1,m}=\frac{q_s x}{(\rho c_p u_a)_1 D_1\left[\begin{matrix}2(1+\kappa)+\\D(\xi_b+\xi_t)\end{matrix}\right]}\left(D(\xi_b+\xi_t)[1+(1+\kappa)\theta_c]+\kappa+1+D(\xi_b-\kappa\xi_t)\left[\frac{(1+\kappa)\left[\theta_c+\Phi_1\left(1+\frac{1}{D}\right)^2\right]+\frac{1}{D}+1}{(1+\kappa)\mathrm{Bi}_1\left(1+\frac{1}{D}\right)^2}\right]\times\left[1-\frac{e^{\lambda}+e^{\lambda/D}}{1+e^{\lambda(1+(1/D))}}\right]\right)+\frac{(1-\varepsilon_1)\dot{q}_{\mathrm{gen},1}}{(\rho c_p u_a)_1}x+T_{a,1} \tag{72}$$

$$T_{b,2,m}=\frac{q_s x}{(\rho c_p u_a)_2 D_2\left[\begin{matrix}2(1+\kappa)+\\D(\xi_b+\xi_t)\end{matrix}\right]}\left(D(\xi_b+\xi_t)[1+(1+\kappa)\theta_c]+\kappa+1+D(\xi_b-\kappa\xi_t)\left[\frac{(1+\kappa)\left[\theta_c+\Phi_1\left(1+\frac{1}{D}\right)^2\right]+\frac{1}{D}+1}{(1+\kappa)\mathrm{Bi}_1\left(1+\frac{1}{D}\right)^2}\right]\times\left[1-\frac{e^{\lambda}+e^{\lambda/D}}{1+e^{\lambda(1+(1/D))}}\right]\right)+\frac{(1-\varepsilon_2)\dot{q}_{\mathrm{gen},2}}{(\rho c_p u_a)_2}x+T_{a,2} \tag{73}$$

$$T_s=\frac{q_s x}{(\rho c_p u_a)_1 D_1(2(1+\kappa)+D(\xi_b+\xi_t))}\left(D(\xi_b+\xi_t)[1+(1+\kappa)\theta_c]+\kappa+1+D(\xi_b-\kappa\xi_t)\left[\frac{(1+\kappa)\left[\theta_c+\Phi_1\left(1+\frac{1}{D}\right)^2\right]+\frac{1}{D}+1}{(1+\kappa)\mathrm{Bi}_1\left(1+\frac{1}{D}\right)^2}\right]\times\left[1-\frac{e^{\lambda}+e^{\lambda/D}}{1+e^{\lambda(1+(1/D))}}\right]\right)-\frac{q_s D_1}{k_{t,\mathrm{eff},1}(1+\kappa)}\left(\Delta\left(\frac{5}{12}-\frac{1}{\mathrm{Bi}_1(1+\kappa)}\left\{1-\frac{2(e^{\lambda}-1)}{\lambda(1+e^{\lambda})}\right\}\right)-\frac{\Phi_1}{\mathrm{Bi}_1}\left\{1-\frac{2(e^{\lambda}-1)}{\lambda(1+e^{\lambda})}\right\}-\frac{\left\{(1+\kappa)\left[\theta_c+\Phi_1\left(1+\frac{1}{D}\right)^2\right]+\frac{1}{D}+1\right\}\left[1-\frac{e^{\lambda}+e^{\lambda/D}}{1+e^{\lambda(1+(1/D))}}\right](e^{\lambda}-1)}{(1+\kappa)\lambda\mathrm{Bi}_1(1+e^{\lambda})\left(1+\frac{1}{D}\right)^2}-\frac{1}{2}\right)+\frac{(1-\varepsilon_1)\dot{q}_{\mathrm{gen},1}}{(\rho c_p u_a)_1}x+T_{a,1} \tag{74}$$

$$\mathrm{Nu}_s=\frac{h_s D_h}{k_{b,\mathrm{eff},1}}=\frac{-2}{\kappa\theta_{b,1,m}}\left(1+\frac{1}{D}\right)$$

$$=\frac{\frac{-2}{\kappa}\left(1+\frac{1}{D}\right)}{\frac{1}{(1+\kappa)}\left(\Delta\left(\frac{5}{12}-\frac{1}{\mathrm{Bi}_1(1+\kappa)}\left\{1-\frac{2(e^{\lambda}-1)}{\lambda(1+e^{\lambda})}\right\}\right)-\frac{\Phi_1}{\mathrm{Bi}_1}\left\{1-\frac{2(e^{\lambda}-1)}{\lambda(1+e^{\lambda})}\right\}-\frac{\left\{(1+\kappa)\left[\theta_c+\Phi_1\left(1+\frac{1}{D}\right)^2\right]+\frac{1}{D}+1\right\}\left[1-\frac{e^{\lambda}+e^{\lambda/D}}{1+e^{\lambda(1+(1/D))}}\right](e^{\lambda}-1)}{(1+\kappa)\lambda\mathrm{Bi}_1(1+e^{\lambda})\left(1+\frac{1}{D}\right)^2}-\frac{1}{2}\right)} \tag{75}$$

where

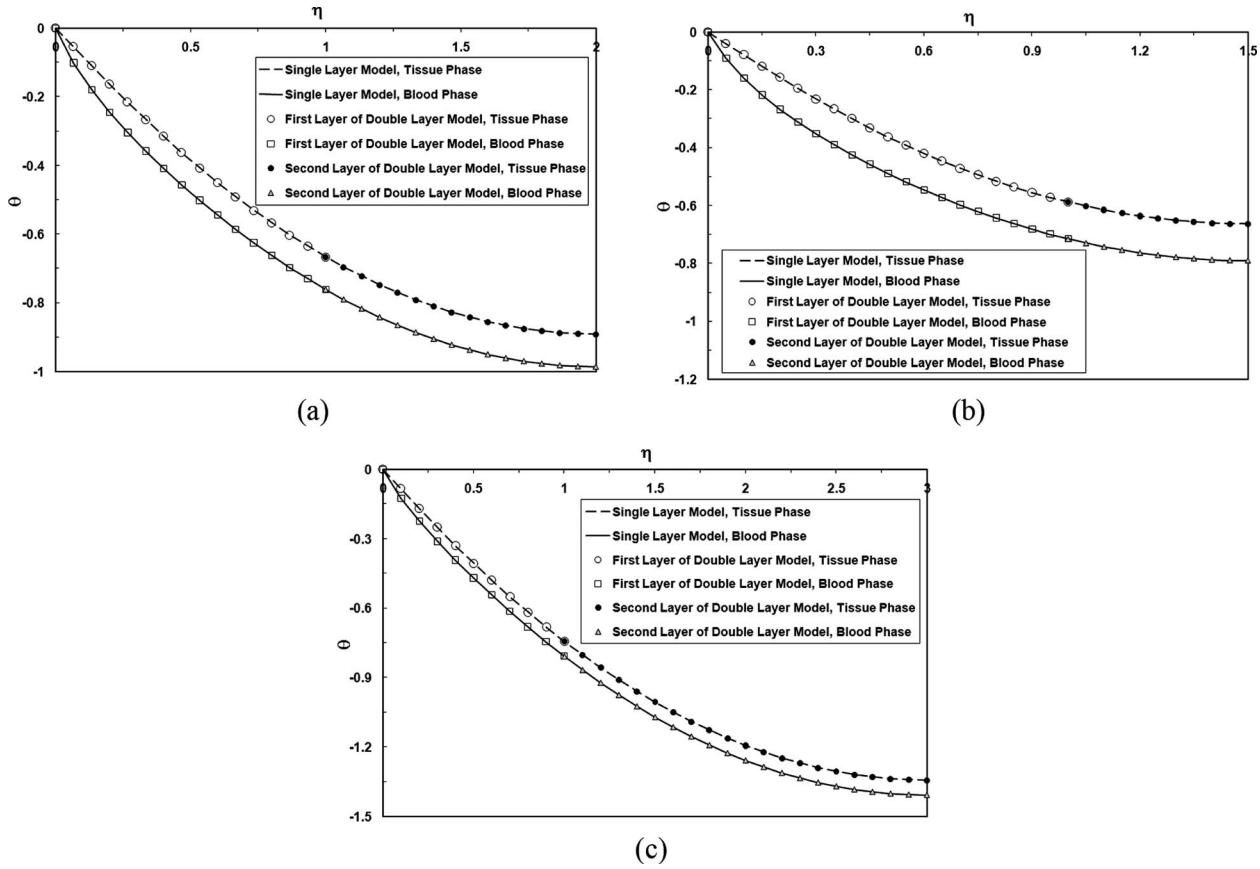

Fig. 2 Comparison of the temperature profiles obtained from double layer analytical solution with similar properties (utilizing two equation modeling) with those obtained from a single layer model [7] for blood and tissue phases with model I (isolated core region) for κ=0.111, ξ_b=0.111, ξ_t=1, $\varepsilon_1=\varepsilon_2$=0.1 and $Bi_1=Bi_2$=10, (*a*) *D*=1, (*b*) *D*=2, and (*c*) *D*=1/2

$$\Delta = \frac{1}{2(1+\kappa)+D(\xi_b+\xi_t)}\left(D(\xi_b+\xi_t)[1+(1+\kappa)\theta_c]+\kappa+1+D(\xi_b-\kappa\xi_t)\left[\frac{(1+\kappa)\left[\theta_c+\Phi_1\left(1+\frac{1}{D}\right)^2\right]+\frac{1}{D}+1}{(1+\kappa)\mathrm{Bi}_1\left(1+\frac{1}{D}\right)^2}\right] \times\left[1-\frac{e^{\lambda}+e^{\lambda/D}}{1+e^{\lambda(1+(1/D))}}\right]\right) \tag{76}$$

2.6 Simplified Solution. A simplified solution can be obtained by assuming thermal equilibrium between the blood and tissue phases, i.e., $\theta_1=\theta_{b,1}=\theta_{t,1}$ and $\theta_2=\theta_{b,2}=\theta_{t,2}$. Adding the energy equations and utilizing the boundary conditions (Eqs. (15)–(32)), and following the same procedure described for the nonequilibrium model, the blood and tissue temperature distributions and the Nusselt number are obtained as follows:

For model I (isolated core region):

$$\theta_{b,1}=\theta_{t,1}=\frac{\eta}{1+\kappa}([1+(1+\kappa)\theta_i]\eta-1) \tag{77}$$

$$\theta_{b,2}=\theta_{t,2}=\frac{1+2(1+\kappa)\theta_i}{2(\xi_b+\xi_t)}\left\{D\left(-\eta+2\left(1+\frac{1}{D}\right)\right)\eta-D-2\right\}+\theta_i \tag{78}$$

where

$$\theta_i=\frac{(\rho c_p u_a)_1 D_1[-q_s+\dot{q}_{\mathrm{gen},2}(1-\varepsilon_2)D_2]-(\rho c_p u_a)_2 D_2[2q_s+\dot{q}_{\mathrm{gen},1}(1-\varepsilon_1)D_1]}{2q_s(1+\kappa)[(\rho c_p u_a)_1 D_1+(\rho c_p u_a)_2 D_2]} \tag{79}$$

and

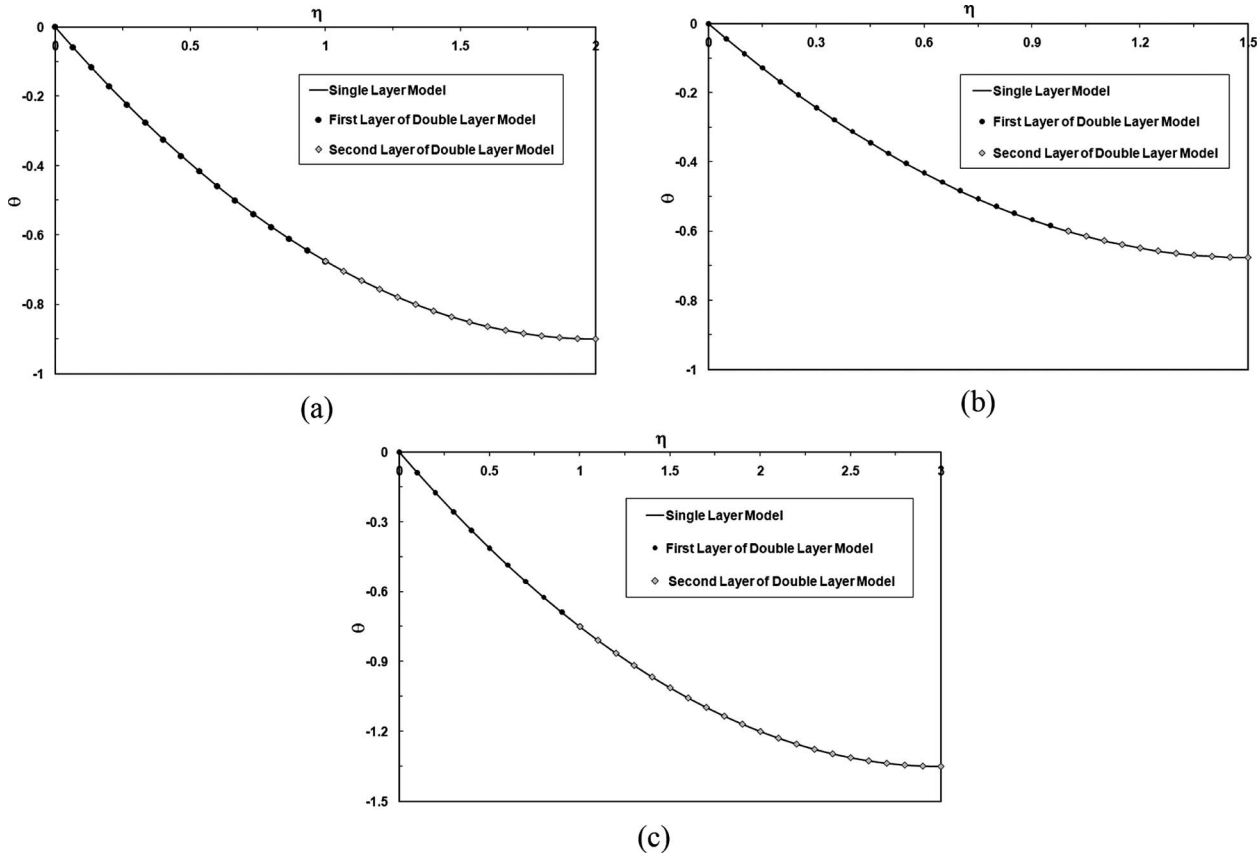

Fig. 3 Comparison of the temperature profiles obtained from double layer analytical solution with similar properties (utilizing one equation modeling) with those obtained from a single layer model [7], for model I (isolated core region) with κ=0.111, ξ_b=0.111, ξ_t=1, $\varepsilon_1=\varepsilon_2$=0.1 and $Bi_1=Bi_2$=10, (*a*) *D*=1, (*b*) *D*=2, and (*c*) *D*=1/2

$$\theta_{b,1,m} = \frac{1}{3}\theta_i - \frac{1}{6(1+\kappa)} \tag{80}$$

$$\theta_{b,2,m} = \left(1 + \frac{2(1+\kappa)}{3(\xi_b+\xi_t)D}\right)\theta_i + \frac{1}{3(\xi_b+\xi_t)D} \tag{81}$$

$$T_{1,m} = \frac{q_s + \dot{q}_{\text{gen},1}(1-\varepsilon_1)D_1 + \dot{q}_{\text{gen},2}(1-\varepsilon_2)D_2}{(\rho c_p u_a)_1 D_1 + (\rho c_p u_a)_2 D_2}x + T_{a,1} \tag{82}$$

$$T_{2,m} = \frac{q_s + \dot{q}_{\text{gen},1}(1-\varepsilon_1)D_1 + \dot{q}_{\text{gen},2}(1-\varepsilon_2)D_2}{(\rho c_p u_a)_1 D_1 + (\rho c_p u_a)_2 D_2}x + T_{a,2} \tag{83}$$

$$\begin{aligned} T_s = {} & \frac{q_s + D_1(1-\varepsilon_1)\dot{q}_{\text{gen},1} + \dot{q}_{\text{gen},2}(1-\varepsilon_2)D_2}{(\rho c_p u_a)_1 D_1 + (\rho c_p u_a)_2 D_2}x + \frac{q_s D_1}{6(1+\kappa)k_{t,\text{eff},1}} + T_{a,1} \\ & - \frac{D_1}{3k_{t,\text{eff},1}}\left(\frac{(\rho c_p u_a)_1 D_1[-q_s + \dot{q}_{\text{gen},2}(1-\varepsilon_2)D_2] - (\rho c_p u_a)_2 D_2[2q_s + \dot{q}_{\text{gen},1}(1-\varepsilon_1)D_1]}{2(1+\kappa)[(\rho c_p u_a)_1 D_1 + (\rho c_p u_a)_2 D_2]}\right) \end{aligned} \tag{84}$$

$$\text{Nu}_s = \frac{h_s D_h}{k_{b,\text{eff},1}} = \frac{-2}{\kappa\theta_{b,1,m}}\left(1 + \frac{1}{D}\right) = \frac{12q_s\dfrac{(1+\kappa)}{\kappa}[(\rho c_p u_a)_1 D_1 + (\rho c_p u_a)_2 D_2]\left(1 + \dfrac{1}{D}\right)}{(\rho c_p u_a)_1 D_1[2q_s - \dot{q}_{\text{gen},2}(1-\varepsilon_2)D_2] + (\rho c_p u_a)_2 D_2[3q_s + \dot{q}_{\text{gen},1}(1-\varepsilon_1)D_1]} \tag{85}$$

and for model II (uniform core temperature):

$$\theta_{b,1} = \theta_{t,1} = \frac{\eta}{1+\kappa}\left([1 + (1+\kappa)\theta_i]\left(\frac{\eta+1}{2}\right) - 1\right) \tag{86}$$

$$\theta_{b,2} = \theta_{t,2} = \frac{D\eta(\eta-2)}{2}\left(D(\theta_c-\theta_i) - \frac{1+\kappa}{\xi_b+\xi_t}\theta_i\right) + \frac{\eta}{2}\left(D(\theta_c-\theta_i) + \frac{1+\kappa}{\xi_b+\xi_t}\theta_i\right) + \frac{D(D-1)}{2}(\theta_c-\theta_i) + \left(1 - \frac{1+D}{2}\frac{1+\kappa}{\xi_b+\xi_t}\right)\theta_i \quad (87)$$

where

$$\theta_i = \frac{D(\xi_b+\xi_t)\theta_c - 1}{D(\xi_b+\xi_t) + 2(1+\kappa)} \quad (88)$$

and

$$\theta_{b,1,m} = \frac{5}{12}\theta_i - \frac{1}{12(1+\kappa)} \quad (89)$$

$$\theta_{b,2,m} = \frac{5}{12}\theta_c + \left(\frac{7}{12} + \frac{1+\kappa}{12D(\xi_b+\xi_t)}\right)\theta_i \quad (90)$$

$$T_{1,m} = \frac{1}{(\rho c_p u_a)_1 D_1}\left(\frac{D(\xi_b+\xi_t)\theta_c - 1}{D(\xi_b+\xi_t) + 2(1+\kappa)} q_s(1+\kappa) + q_s + \dot{q}_{\text{gen},1}(1-\varepsilon_1)D_1\right)x + T_{a,1} \quad (91)$$

$$T_{2,m} = \frac{1}{(\rho c_p u_a)_2 D_2} \times \left(\frac{1 - D(\xi_b+\xi_t)\theta_c}{D(\xi_b+\xi_t) + 2(1+\kappa)} q_s[D(\xi_b+\xi_t) + \kappa + 1] + q_s D(\xi_b+\xi_t)\theta_c + \dot{q}_{\text{gen},2}(1-\varepsilon_2)D_2\right)x + T_{a,2} \quad (92)$$

$$T_s = \frac{x}{(\rho c_p u_a)_1 D_1}\left(\frac{q_s(1+\kappa)(D(\xi_b+\xi_t)\theta_c - 1)}{D(\xi_b+\xi_t) + 2(1+\kappa)} + q_s + \dot{q}_{\text{gen},1}(1-\varepsilon_1)D_1\right) + \frac{q_s D_1}{12k_{t,\text{eff},1}}\left(\frac{5\{1 - D(\xi_b+\xi_t)\theta_c\}}{D(\xi_b+\xi_t) + 2(1+\kappa)} + \frac{1}{1+\kappa}\right) + T_{a,1} \quad (93)$$

$$\text{Nu}_s = \frac{h_s D_h}{k_{b,\text{eff},1}} = \frac{-2}{\kappa\theta_{b,1,m}}\left(1 + \frac{1}{D}\right) = \frac{\frac{-24}{\kappa}\left(1 + \frac{1}{D}\right)}{\frac{5(D(\xi_b+\xi_t)\theta_c - 1)}{D(\xi_b+\xi_t) + 2(1+\kappa)} - \frac{1}{1+\kappa}} \quad (94)$$

3 Results and Discussions

The presented analytical expressions allow for incorporating variations in the representative volume fraction as well as various physical attributes. Comparing temperature profiles for any of the single layers with the available data in the literature provided detailed validations. Exact solutions for forced convective flow through a channel filled with a porous medium and subject to an imposed heat flux (which is equivalent to the isolated core region model without a metabolic heat generation) were presented in the works of Lee and Vafai [33] and Marafie and Vafai [37]. As such, the tissue and blood temperature profiles were compared with analytical correlations obtained by Lee and Vafai [33]. The temperature distributions were found to be in excellent agreement for both phases with the results presented by Lee and Vafai [33] for a variety of blood-tissue interstitial heat exchange parameters. The blood and tissue temperature profiles were also found to be in excellent agreement with the analytical and numerical results of Marafie and Vafai [37]. Numerical results based on an implicit, pressure-based, cell-centered finite volume method, second order upwinding and under relaxation, was also compared with the obtained analytical temperature distribution for single layer model for both isolated and uniform core temperature condition models. These comparisons were found to be in excellent agreement and were presented in some detail in the works of Mahjoob and Vafai [7]. The temperature profiles obtained from the present analytical correlations can effectively predict the tissue and blood temperatures. The temperature distribution is very crucial for an effective thermal therapy such as hyperthermia cancer treatment. Based on the cited values in the literature [26], a typical volume fraction of 0.1 for the vascular system is utilized. However, the present established analytical expressions allow for incorporating variations in the representative volume fraction as well as various physical attributes. Figures 2(*a*)–2(*c*) represent the blood and tissue temperature profiles for a dual layer region, incorporating isolated core region for different layer thickness ratio (D). Since the physical properties of both layers is the same, the profiles have been compared with the profiles obtained from the exact solutions for a single layer with equivalent properties [7]. The comparison indi-

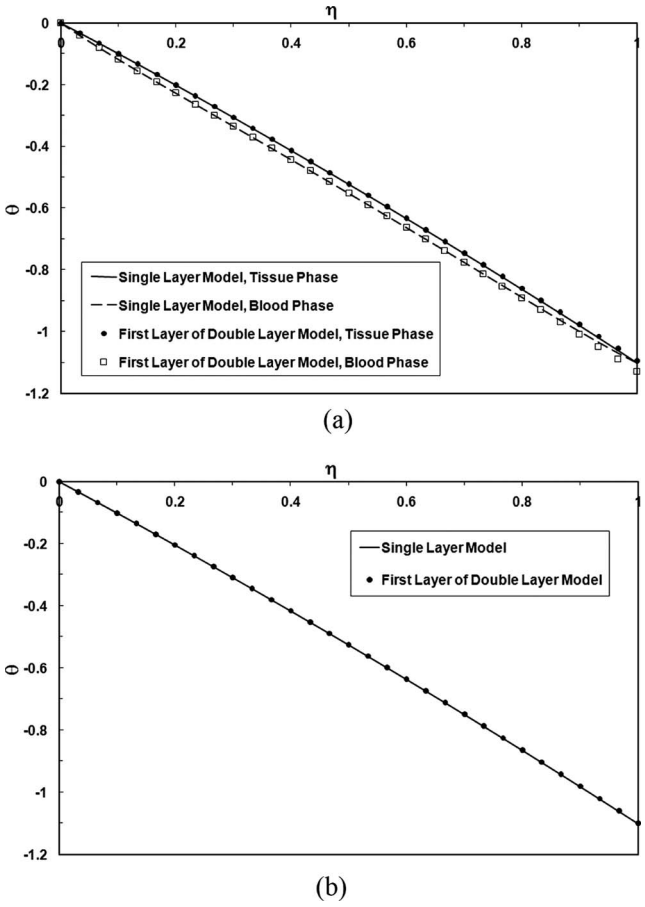

Fig. 4 Comparison of the temperature profiles obtained from the first layer of the double layer analytical solution with those obtained from a single layer model [7] for model II (uniform core temperature) with κ=0.111, ξ_b=0.111, ξ_t=1, $\varepsilon_1=\varepsilon_2$=0.1, and $\text{Bi}_1=\text{Bi}_2$=10, utilizing (*a*) two equation and (*b*) one equation models

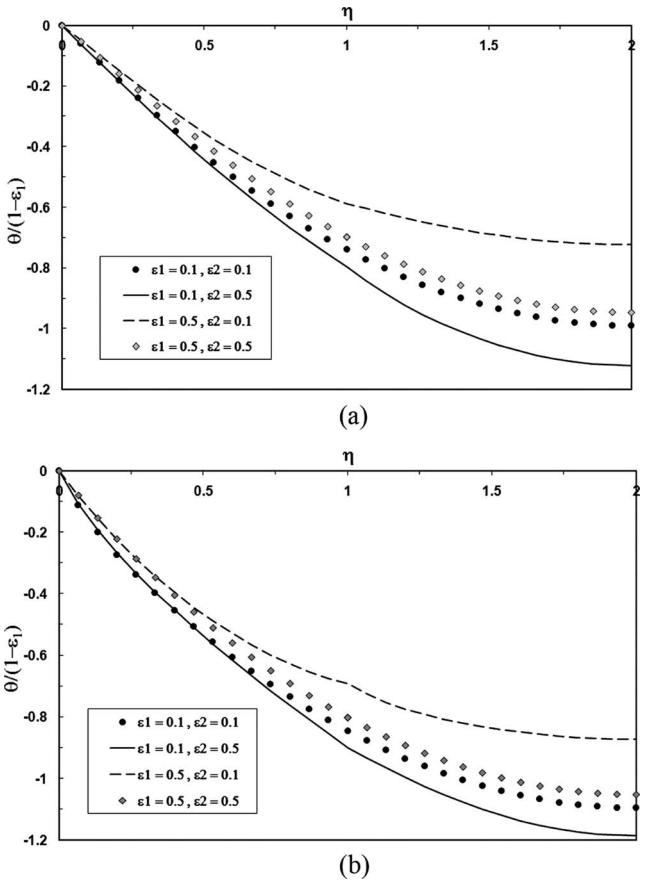

Fig. 5 The effect of vascular volume fraction variation in biological layers, for model I (isolated core region), for similar blood and tissue properties in the layers, $D=1$, $Bi_1=Bi_2=10$, $\Phi_1/(1-\varepsilon_1)=\Phi_2/(1-\varepsilon_2)=0.55$, (*a*) tissue phase, (*b*) blood phase

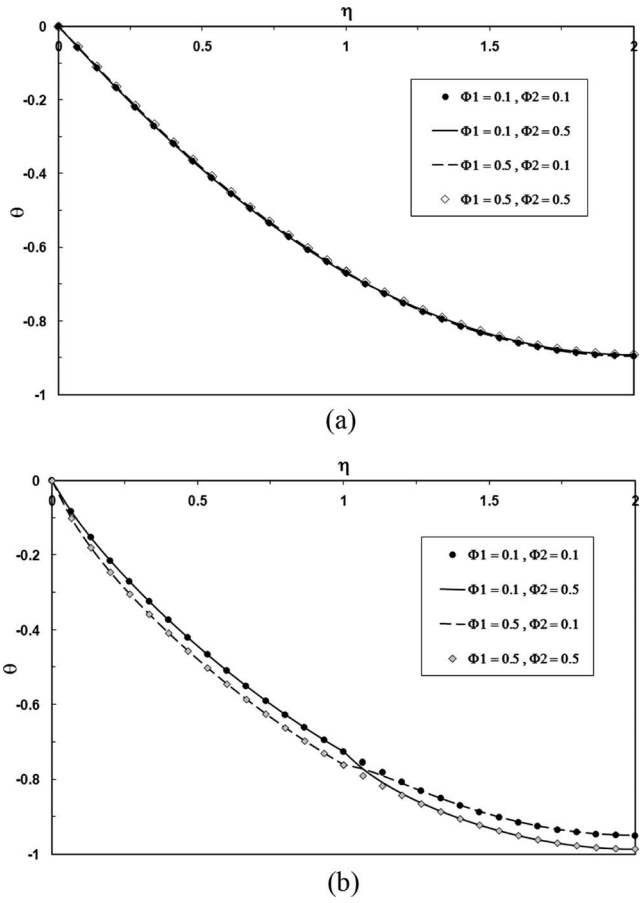

Fig. 6 The effect of metabolic heat generation in biological layers, for model I (isolated core region), for similar blood and tissue properties in the layers, $D=1$, $\kappa=0.111$, $\xi_b=0.111$, $\xi_t=1$, $\varepsilon_1=\varepsilon_2=0.1$, $Bi_1=Bi_2=10$, (*a*) tissue phase, (*b*) blood phase

cates an excellent agreement in all cases. In Figs. 3(*a*)–3(*c*), the temperature profiles for each layer of the double layer analytical solution (utilizing one equation model) are compared with those obtained for the single layer model [7], for model I (isolated core region), under equivalent conditions. The comparisons also indicate a very good agreement.

The temperature profiles obtained from model II (uniform core temperature) are presented in Fig. 4. Tissue and blood temperature profiles obtained for the first of the double layer analytical solution (utilizing the two equation model) are compared with those obtained for the single layer model [7] under the equivalent conditions. The comparison displays a very good agreement. Comparison is also done for the case of one equation model, further validating the present analytical solution (Fig. 4(*b*)).

Figure 5 displays the effect of vascular volume fraction on the blood and tissue temperature profiles in a dual layer biological media. An increase in the volume fraction, in the cases with uniform vascular volume fraction in both layers, results in a more uniform temperature profile through the layers, possibly leading to a more effective hyperthermia treatment. It should be noted that a change in the vascular volume fraction also translates in a change in the blood and tissue effective thermal conductivities. The body regulates the temperature during hyperthermia treatment by utilizing the arterial blood, while modifying the vascular volume fraction of the biological structure. The natural body thermal regulation system increases or decreases the vascular volume fraction of the biological structure when exposed to a higher or lower temperature, respectively. The physical attributes obtained from this analytical solution can be used to improve the efficiency of thermal therapy techniques. An increase in the vascular volume fraction of the second layer increases the nonuniformity in temperature profiles. However, the tissue and blood temperature uniformity is more prominently affected by the vascular volume fraction of the first layer, which is subject to the imposed heat flux.

Figure 6 represents the effect of metabolic heat generation on the blood and tissue temperature profiles. As can be seen the metabolic heat generation has more pronounced effect on the nondimensional blood phase since temperature rise in the tissue phase and organ's surface is higher than that of the blood phase. As such, a larger heat generation ratio results in higher temperatures in the organ as well as the blood within it and more distinct temperature nonuniformity. The effect of variable heat generation on the biological layers is also presented in Fig. 6. In the previous works by authors, the effects of thermal conductivities of the tissue and blood phases and the nondimensional Biot number (Bi) have been discussed extensively [7,33,48–50].

4 Conclusions

A detailed analysis of bioheat transport through dual layer biological media is presented in this work for the first time. These analytical solutions enable an understanding of heat transfer processes and temperature distributions within biological media, which are key issues in thermal therapy techniques. The comprehensive analytical solutions represent the blood and tissue temperature distributions as well as the Nusselt number correlations for two primary conditions, namely, isolated core region and uniform core temperature. The analytical solutions encompass various pertinent parameters such as the volume fraction of the vas-

cular system, the blood and tissue thermal conductivities, interfacial blood-tissue heat exchange, metabolic heat generation, tissue/organ depth, arterial velocity and temperature, body core temperature, imposed hyperthermia heat flux, and the blood's physical properties. Analytical solutions are also presented for a simplified case corresponding to local thermal equilibrium between the blood and tissue phases. The comparisons, utilizing both local thermal nonequilibrium and equilibrium assumptions, indicate an excellent agreement. The effect of the variable vascular volume fraction and metabolic heat generation within the biological media is also discussed.

Nomenclature

a_{tb} = specific surface area (m^{-1})
Bi = Biot number, $h_{tb}a_{tb}D_1^2/k_{t,\mathrm{eff},1}$
c_p = blood specific heat ($J\,kg^{-1}\,K^{-1}$)
D_1 = depth of the first layer of tissue/organ (m)
D_2 = depth of the second layer of tissue/organ (m)
D = nondimensional parameter for depth, D_1/D_2
D_h = hydraulic diameter of the channel, $2(D_1+D_2)$ (m)
h_{tb} = blood-tissue interstitial heat transfer coefficient ($W\,m^{-2}\,K^{-1}$)
h_s = surface heat transfer coefficient for the thermal nonequilibrium model, $q_s/(T_s\text{-}T_{b,m,1})$ ($W\,m^{-2}\,K^{-1}$)
$k_{b,\mathrm{eff}}$ = effective thermal conductivity of the blood phase ($W\,m^{-1}\,K^{-1}$)
$k_{t,\mathrm{eff}}$ = effective thermal conductivity of the tissue phase ($W\,m^{-1}\,K^{-1}$)
Nu_s = Nusselt number at the organ's surface
q = heat flux ($W\,m^{-2}$)
q_s = heat flux at the body organ surface ($W\,m^{-2}$)
$\dot{q}_{\mathrm{gen}}$ = heat generation within the biological tissue ($W\,m^{-3}$)
T = temperature (K)
T_a = arterial blood temperature entering the organ (K)
$T_{b,m}$ = blood mean temperature (K)
T_c = body core temperature (K)
T_s = temperature of the body organ surface subject to an imposed heat flux (K)
u_a = arterial blood velocity entering the tissue layer ($m\,s^{-1}$)
x = longitudinal coordinate (m)
y = transverse coordinate (m)

Greek Symbols

η = nondimensional transverse coordinate, y/D_1
Φ = nondimensional heat generation within the biological tissue, $(1-\varepsilon)D_1\dot{q}_{\mathrm{gen}}/q_s$
κ = ratio of the effective blood thermal conductivity to that of the tissue in the first layer, $k_{b,\mathrm{eff},1}/k_{t,\mathrm{eff},1}$
ρ = blood density ($kg\,m^{-3}$)
ξ_b = nondimensional effective blood thermal conductivity of the second layer, $k_{b,\mathrm{eff},2}/k_{t,\mathrm{eff},1}$
ξ_t = nondimensional effective tissue thermal conductivity of the second layer, $k_{t,\mathrm{eff},2}/k_{t,\mathrm{eff},1}$
λ = parameter, $\sqrt{\mathrm{Bi}_1(1+\kappa)/\kappa}$
λ' = parameter, $\sqrt{(\xi_b+\xi_t)\mathrm{Bi}_2/\xi_b\xi_t}$
θ = nondimensional temperature, $k_{t,\mathrm{eff},1}(T-T_s)/q_sD_1$
$\theta_{b,m}$ = nondimensional blood mean temperature
θ_c = nondimensional body core temperature, $k_{t,\mathrm{eff},1}(T_c-T_s)/q_sD_1$
$\Delta\theta$ = nondimensional temperature difference between tissue and blood phases
ω = blood perfusion rate (s^{-1})

Subscripts/Superscripts

1 = first layer
2 = second layer
B = blood phase
b,m = blood mean
c = body core
eff = effective property
j = indicator
s = body organ surface subject to an imposed heat flux
t = tissue phase

Symbol

$\langle\,\rangle$ = intrinsic volume average of a quantity

References

[1] Oleson, J. R., Dewhirst, M. W., Harrelson, J. M., Leopold, K. A., Samulski, T. V., and Tso, C. Y., 1989, "Tumor Temperature Distributions Predict Hyperthermia Effect," Int. J. Radiat. Oncol. Biol. Phys., **16**(3), pp. 559–70.
[2] Field, S. B., and Hand, J. W., 1990, *An Introduction to the Practical Aspects of Clinical Hyperthermia*, Taylor & Francis, New York.
[3] Diederich, C. J., 2005, "Thermal Ablation and High-Temperature Thermal Therapy: Overview of Technology and Clinical Implementation," Int. J. Hyperthermia, **21**(8), pp. 745–753.
[4] Wust, P., Hildebrandt, B., Sreenivasa, G., Rau, B., Gellermann, J., Riess, H., Felix, R., and Schlag, P. M., 2002, "Hyperthermia in Combined Treatment of Cancer," Lancet Oncol., **3**(8), pp. 487–497.
[5] Hall, E. J., and Roizin-Towle, L., 1984, "Biological Effects of Heat," Cancer Res., **44**, pp. 4708s–4713s.
[6] Field, S. B., 1987, "Hyperthermia in the Treatment of Cancer," Phys. Med. Biol., **32**(7), pp. 789–811.
[7] Mahjoob, S., and Vafai, K., 2009, "Analytical Characterization of Heat Transfer Through Biological Media Incorporating Hyperthermia Treatment," Int. J. Heat Mass Transfer, **52**(5–6), pp. 1608–1618.
[8] Urano, M., 1999, "For the Clinical Application of Thermochemotherapy Given at Mild Temperatures," Int. J. Hyperthermia, **15**(2), pp. 79–107.
[9] van der Zee, J., González González, D., van Rhoon, G. C., van Dijk, J. D. P., van Putten, W. L. J., and Hart, A. A. M., 2000, "Comparison of Radiotherapy Alone With Radiotherapy Plus Hyperthermia in Locally Advanced Pelvic Tumours: A Prospective, Randomised, Multicentre Trial," Lancet, **355**(9210), pp. 1119–1125.
[10] Pennes, H. H., 1948, "Analysis of Tissue and Arterial Blood Temperature in the Resting Human Forearm," J. Appl. Physiol., **1**, pp. 93–122.
[11] Charny, C. K., 1992, "Mathematical Models of Bioheat Transfer," Adv. Heat Transfer, **22**, pp. 19–155.
[12] Wulff, W., 1974, "The Energy Conservation Equation for Living Tissue," IEEE Trans. Biomed. Eng., **BME-21**(6), pp. 494–495.
[13] Klinger, H. G., 1974, "Heat Transfer in Perfused Biological Tissue—I: General Theory," Bull. Math. Biol., **36**(4), pp. 403–415.
[14] Chen, M. M., and Holmes, K. R., 1980, "Microvascular Contributions in Tissue Heat Transfer," Ann. N.Y. Acad. Sci., **335**, pp. 137–150.
[15] Weinbaum, S., Jiji, L. M., and Lemons, D. E., 1984, "Theory and Experiment for the Effect of Vascular Microstructure on Surface Tissue Heat Transfer. Part I. Anatomical Foundation and Model Conceptualization," ASME J. Biomech. Eng., **106**(4), pp. 321–330.
[16] Jiji, L. M., Weinbaum, S., and Lemons, D. E., 1984, "Theory and Experiment for the Effect of Vascular Microstructure on Surface Tissue Heat Transfer—Part II: Model Formulation and Solution," ASME J. Biomech. Eng., **106**(4), pp. 331–341.
[17] Weinbaum, S., and Jiji, L. M., 1985, "A New Simplified Bioheat Equation for the Effect of Blood Flow on Local Average Tissue Temperature," ASME J. Biomech. Eng., **107**(2), pp. 131–139.
[18] Mitchell, J. W., and Myers, G. E., 1968, "An Analytical Model of the Countercurrent Heat Exchange Phenomena," Biophys. J., **8**, pp. 897–911.
[19] Keller, K. H., and Seilder, L., 1971, "An Analysis of Peripheral Heat Transfer in Man," J. Appl. Physiol., **30**(5), pp. 779–789.
[20] Chen, C., and Xu, L. X., 2003, "A Vascular Model for Heat Transfer in an Isolated Pig Kidney During Water Bath Heating," ASME J. Heat Transfer, **125**(5), pp. 936–943.
[21] Baish, J. W., Ayyaswamy, P. S., and Foster, K. U., 1986, "Small Scale Temperature Fluctuations in Perfused Tissue During Local Hyperthermia," ASME J. Biomech. Eng., **108**(3), pp. 246–250.
[22] Baish, J. W., Ayyaswamy, P. S., and Foster, K. R., 1986, "Heat Transport Mechanisms in Vascular Tissues: A Model Comparison," ASME J. Biomech. Eng., **108**(4), pp. 324–331.
[23] Abraham, J. P., and Sparrow, E. M., 2007, "A Thermal-Ablation Bioheat Model Including Liquid-to-Vapor Phase Change, Pressure- and Necrosis-

Dependent Perfusion, and Moisture-Dependent Properties," Int. J. Heat Mass Transfer, **50**(13–14), pp. 2537–2544.
[24] Arkin, H., Xu, L. X., and Holmes, K. R., 1994, "Recent Developments in Modeling Heat Transfer in Blood Perfused Tissues," IEEE Trans. Biomed. Eng., **41**, pp. 97–107.
[25] Chato, J. C., 1980, "Heat Transfer to Blood Vessels," ASME J. Biomech. Eng., **102**(2), pp. 110–118.
[26] Khanafer, K., and Vafai, K., 2009, "Synthesis of Mathematical Models Representing Bioheat Transport," *Advance in Numerical Heat Transfer*, Vol. 3, W. J. Minkowycz and E. M. Sparrow, eds., Taylor & Francis, London, pp. 1–28.
[27] Nakayama, A., and Kuwahara, F., 2008, "A General Bioheat Transfer Model Based on the Theory of Porous Media," Int. J. Heat Mass Transfer, **51**(11–12), pp. 3190–3199.
[28] Khaled, A. R., and Vafai, K., 2003, "The Role of Porous Media in Modeling Flow and Heat Transfer in Biological Tissues," Int. J. Heat Mass Transfer, **46**, pp. 4989–5003.
[29] Vafai, K., and Tien, C. L., 1981, "Boundary and Inertia Effects on Flow and Heat Transfer in Porous Media," Int. J. Heat Mass Transfer, **24**, pp. 195–203.
[30] Sozen, M., and Vafai, K., 1990, "Analysis of the Non-Thermal Equilibrium Condensing Flow of a Gas Through a Packed Bed," Int. J. Heat Mass Transfer, **33**, pp. 1247–1261.
[31] Vafai, K., and Sozen, M., 1990, "Analysis of Energy and Momentum Transport for Fluid Flow Through a Porous Bed," ASME J. Heat Transfer, **112**, pp. 690–699.
[32] Quintard, M., and Whitaker, S., 2000, "Theoretical Analysis of Transport in Porous Media," *Handbook of Porous Media*, K. Vafai, ed., Marcel Dekker Inc., New York, pp. 1–52.
[33] Lee, D. Y., and Vafai, K., 1999, "Analytical Characterization and Conceptual Assessment of Solid and Fluid Temperature Differentials in Porous Media," Int. J. Heat Mass Transfer, **42**, pp. 423–435.
[34] Amiri, A., and Vafai, K., 1994, "Analysis of Dispersion Effects and Nonthermal Equilibrium, Non-Darcian, Variable Porosity Incompressible Flow Through Porous Medium," Int. J. Heat Mass Transfer, **37**, pp. 939–954.
[35] Alazmi, B., and Vafai, K., 2002, "Constant Wall Heat Flux Boundary Conditions in Porous Media Under Local Thermal Non-Equilibrium Conditions," Int. J. Heat Mass Transfer, **45**, pp. 3071–3087.
[36] Amiri, A., Vafai, K., and Kuzay, T. M., 1995, "Effect of Boundary Conditions on Non-Darcian Heat Transfer Through Porous Media and Experimental Comparisons," Numer. Heat Transfer, Part A, **27**, pp. 651–664.
[37] Marafie, A., and Vafai, K., 2001, "Analysis of Non-Darcian Effects on Temperature Differentials in Porous Media," Int. J. Heat Mass Transfer, **44**, pp. 4401–4411.
[38] Jiang, S. C., Ma, N., Li, H. J., and Zhang, X. X., 2002, "Effects of Thermal Properties and Geometrical Dimensions on Skin Burn Injuries," Burns, **28**(8), pp. 713–717.
[39] Wang, H., Dai, W., and Bejan, A., 2007, "Optimal Temperature Distribution in a 3D Triple-Layered Skin Structure Embedded With Artery and Vein Vasculature and Induced by Electromagnetic Radiation," Int. J. Heat Mass Transfer, **50**(9–10), pp. 1843–1854.
[40] Ma, N., Gao, X., and Zhang, X. X., 2004, "Two-Layer Simulation Model of Laser-Induced Interstitial Thermo-Therapy," Lasers Med. Sci., **18**, pp. 184–189.
[41] Khakpour, M., and Vafai, K., 2008, "A Critical Assessment of Arterial Transport Models," Int. J. Heat Mass Transfer, **51**, pp. 807–822.
[42] Curry, F. E., 1984, "Mechanics and Thermodynamics of Transcapillary Exchange," *Handbook of Physiology*, E. M. Renkin, ed., American Physiological Society, Bethesda, MD, Vol. IV, Chap. 8.
[43] Ogston, A. G., 1958, "The Spaces in a Uniform Random Suspension of Fibers," Trans. Faraday Soc., **54**, pp. 1754–1757.
[44] Ogston, A. G., Preston, B. N., and Wells, J. D., 1973, "On the Transport of Compact Particles Through Solutions of Chain-Polymer," Proc. R. Soc. London, Ser. A, **333**, pp. 297–316.
[45] Schnitzer, J. E., 1988, "Analysis of Steric Partition Behavior of Molecules in Membranes Using Statistical Physics. Application to Gel Chromatography and Electrophoresis," Biophys. J., **54**, pp. 1065–1076.
[46] Yuan, F., Chien, S., and Weinbaum, S., 1991, "A New View of Convective-Diffusive Transport Processes in the Arterial Intima," ASME J. Biomech. Eng., **113**(3), pp. 314–329.
[47] Huang, Y., Rumschitzki, D., Chien, S., and Weinbaum, S., 1994, "A Fiber Matrix Model for the Growth of Macromolecular Leakage Spots in the Arterial Intima," ASME J. Biomech. Eng., **116**, pp. 430–445.
[48] Mahjoob, S., and Vafai, K., 2009, "Analytical Characterization and Production of an Isothermal Surface for Biological and Electronics Applications," ASME J. Heat Transfer, **131**(5), p. 052604.
[49] Mahjoob, S., and Vafai, K., 2008, "A Synthesis of Fluid and Thermal Transport Models for Metal Foam Heat Exchangers," Int. J. Heat Mass Transfer, **51**(15–16), pp. 3701–3711.
[50] Mahjoob, S., Vafai, K., and Beer, N. R., 2008, "Rapid Microfluidic Thermal Cycler for Polymerase Chain Reaction Nucleic Acid Amplification," Int. J. Heat Mass Transfer, **51**(9–10), pp. 2109–2122.